

The 24-Micron View of Embedded Star Formation in NGC 7129

J. Muzerolle ¹, S. T. Megeath ², R. A. Gutermuth ³, L. E. Allen ², J. L. Pipher ³, L. Hartmann ², K. D. Gordon ¹, D. L. Padgett ⁵, A. Noriega-Crespo ⁵, P. C. Myers ², G. G. Fazio ², G. H. Rieke ¹, E. T. Young ¹, J. E. Morrison ¹, D. C. Hines ^{1,4}, K. Y. L. Su ¹, C. W. Engelbracht ¹, & K. A. Misselt ¹

ABSTRACT

We present observations of the star formation region NGC 7129 taken with the Multiband Imaging Photometer for *Spitzer* (MIPS). A significant population of sources, likely pre-main sequence members of the young stellar cluster, is revealed outside the central photoionization region. Combining with Infrared Array Camera (IRAC) and ground-based near-infrared images, we have obtained colors and spectral energy distributions for some 60 objects. The [3.6]-[4.5] vs. [8]-[24] color-color plane shows sources clustered at several different loci, which roughly correspond to the archetypal evolutionary sequence Class 0, I, II, and III. We obtain preliminary classifications for 36 objects, and find significant numbers of both Class I and II objects. Most of the pre-main sequence candidates are associated with the densest part of the molecular cloud surrounding the photoionization region, indicating active star formation over a broad area outside the central cluster. We discuss three Class II candidates that exhibit evidence of inner disk clearing, which would be some of the youngest known examples of a transition from accretion to optically thin quiescent disks.

Subject headings: pre-main sequence — stars: formation — infrared: stars

¹Steward Observatory, University of Arizona, 933 N. Cherry Ave., Tucson, AZ 85721 (jamesm@as.arizona.edu)

²Harvard-Smithsonian Center for Astrophysics, Mail Stop 42, 60 Garden Street, Cambridge, MA 02138

³Department of Physics and Astronomy, University of Rochester, Rochester, NY 14627

⁴Space Science Institute, 4750 Walnut Street, Suite 205, Boulder, CO 80301

⁵*Spitzer* Science Center, Caltech, Pasadena, CA 91125

1. Introduction

A complete census of young stellar objects in a wide variety of star forming regions is important to advancing our understanding of star and planet formation processes. The prevailing paradigm places young stellar objects into an evolutionary sequence spanning the first few million years of their existence (Adams et al. 1987): the youngest embedded protostars surrounded by infalling envelopes and growing accretion disks (Class 0/I objects); pre-main sequence (PMS) stars with less active accretion disks (Class II); PMS stars with no disks or optically thin remnant dust (Class III). The characteristics of this evolutionary sequence inform the origins of the initial mass function and the formation and frequency of planetary systems. By studying a large sample of different stellar nurseries, we can begin to examine in detail the effects of the star forming environment on these processes.

Mid-infrared observations are essential for identifying and characterizing excess dust emission from circumstellar envelopes and disks. Previous surveys such as IRAS have been able to study in detail only the nearest star forming regions such as Taurus (e.g. Kenyon et al. 1990; Kenyon & Hartmann 1995) and ρ Oph (e.g. Wilking et al. 1989; Luhman & Rieke 1999), at distances of 140 and 160 pc, respectively. The *Spitzer Space Telescope*, with the combination of unprecedented sensitivity and spatial resolution provided by the Infrared Array Camera (IRAC) and Multiband Imaging Photometer for *Spitzer* (MIPS), has the capability to characterize regions as distant as ~ 1 kpc, significantly increasing the statistics of PMS object properties as a function of stellar environment, mass, and age.

The $24\ \mu\text{m}$ channel of MIPS in particular provides a robust diagnostic of the presence of circumstellar envelopes around Class 0/I objects, whose relatively cold dust emission is characterized by a rising spectral energy distribution (SED) through the mid-infrared. It is also important for probing emission from accretion disks around Class II objects, being most sensitive to structure at $\sim 1 - 5$ AU (the region of gas giant formation in the solar nebula), such as changes in the disk surface height due to dust settling from grain growth (Miyake & Nakagawa 1995). Observations at $24\ \mu\text{m}$ are also essential for identifying inner gaps in disks, as indicated by the lack of dust emission at shorter wavelengths. Such objects are indicative of a transition between the Class II and III stages that may be brought about by grain growth/coagulation in the inner disk. Finally, the $24\ \mu\text{m}$ channel provides the primary means of identifying optically thin dust disks that may be the remnants of earlier accretion activity, or (especially at older ages) “debris” generated by planetesimal collisions.

NGC 7129 offers a prime example of a very young embedded region (~ 1 Myr), with significant molecular material undergoing active star formation. The cloud has already been partially disrupted by winds and photoionization from newly-formed massive stars (Miskolczi et al. 2001), creating a reflection nebula visible in the optical. A significant population of

pre-main sequence objects within the reflection nebula has been indicated by ground-based near-infrared observations (Hodapp 1994); however, a complete census of young objects at all PMS evolutionary phases is lacking. We present MIPS observations of this cluster, focusing on the 24 μm imaging to identify protostellar envelopes and accretion disks, and obtain a preliminary picture of the PMS population outside the central reflection nebula.

2. Observations

The region was mapped with MIPS using scan mode (Rieke et al. 2004), covering a total area of 15' by 30' common to all three detector arrays. The map consists of 6 scan legs with half-array cross-scan offsets, providing the necessary redundancy so that all points on the sky in the region of interest were placed on side “A” of the 70 μm array (Rieke et al.). Medium scan rate was employed, providing a total effective exposure time per pixel of 80 seconds at 24 μm , 40 seconds at 70 μm , and 8 seconds at 160 μm . The data were reduced and mosaicked using the instrument team in-house Data Analysis Tool, which includes per-exposure calibration of all detector transient effects, dark current subtraction, and flat fielding/illumination correction (Gordon et al. 2004). Coaddition and mosaicking of individual frames included applying distortion corrections and cosmic ray rejection. A portion of the final 24 μm mosaic is shown in Figure 1.

3. Results

The 24 μm image of NGC 7129 shows bright extended emission in the center that corresponds to the reflection nebula seen in the optical. The primary sources of photoionization, the B3 stars BD+65 1637 and BD+65 1638, are not detected directly, but extended halos of warm dust are seen at their positions. Known PMS stars LkH α 234 and SVS 13, to the northeast of BD+65 1637, are completely saturated in the PSF core. The previously identified far-infrared source FIRS 2 appears to the south of BD+65 1637; it is slightly saturated in the central pixel. The cluster of pre-main sequence stars located within the reflection nebula (Gutermuth et al. 2004) is largely unseen at 24 μm because of the bright background emission and lower spatial resolution of the instrument. However, a fairly large number of point sources is detected outside the central region, primarily in an arc to the north, east, and south. Since MIPS does not have the sensitivity to detect most stellar photospheres at the distance of NGC 7129 (which we take to be 1 kpc; Racine 1968), most of these sources likely exhibit infrared excesses, which we explore in more detail below.

We measured photometry on point sources using daophot with PSF-fitting (the flux for FIRS 2 was recovered by fitting the PSF wings; the other two saturated sources were unrecoverable). A total of 182 point sources was measured over the entire map at 24 μm , four at 70 μm , and none at 160 μm . The latter two arrays suffer from the very strong extended emission and saturate over large areas, which significantly curtailed the sensitivity to weaker point sources. We thus focus our analysis on the 24 μm data. Typical errors, dominated by uncertainties in the absolute calibration, are within $\sim 10\%$ at 24 μm and $\sim 20\%$ at 70 μm . Finally, fluxes were converted into magnitudes referenced to the Vega-system using a zero-point (7.3 Jy) derived from the Vega spectrum.

We have combined our MIPS measurements with ground-based *JHK* and IRAC 4-channel photometry (see Gutermuth et al. 2004 for details). The observations are not simultaneous, so we are potentially subject to uncertainties from variability; however, emission at the longer wavelengths originates mostly from a larger area of circumstellar material farther from the central star, so we do not expect significant variability at 24 μm . With these data, we can determine infrared colors and construct spectral energy distributions for our sources, and begin to probe the characteristics of the young stellar objects in NGC 7129. Along these lines, we present the ([8]-[24]) vs. ([3.6]-[5.8]) color-color and ([8]-[24]) vs. [24] color-magnitude diagrams in Figure 2 for all sources detected in these bands. The ([8]-[24]) color in particular is very sensitive to excesses, since photospheric colors should be close to zero for all spectral types.

Figure 2 shows that almost all the sources plotted have a significant infrared excess. A small group of 6 sources is clustered around ([3.5]-[5.8]) ~ 0 , $0 \lesssim ([8] - [24]) \lesssim 1$, and is probably a mixture of pure photospheres and perhaps weak 24 μm excesses. The remainder of the sources have strong ([8]-[24]) excesses and moderate-to-strong ([3.5]-[5.8]) excesses; these are likely to be Class I objects with envelopes or Class II objects with optically thick disks. The source with the most extreme colors corresponds to FIRS 2, an outflow source and probably a Class 0 protostar given its cold, massive envelope as seen at *mm* wavelengths (Eiroa et al. 1998) (however, we caution that much of the flux in the IRAC bands may be contaminated by shocked emission from the outflow). There is an interesting gap at ([8]-[24]) $\sim 1 - 2.5$, which suggests a lack of objects having remnant disks with inner regions that are no longer optically thick in the infrared.

A more detailed look at the spectral energy distributions is required to better disentangle the object classifications. In Figure 3, we show typical SEDs spanning the range of characteristics of our total sample; coordinates and magnitudes for these sources are listed in Table 1. Class I objects are characterized by a rising SED through near- and mid-infrared wavelengths, typically peaking at 60-100 μm (Lada 1987). The top panel of Figure 3 shows 4

such objects (including $70\ \mu\text{m}$ measurements, at which wavelength the SEDs are still rising). The SED of a known Class I object in Taurus, L1551-IRS5, is shown for comparison. The lower panel shows examples of candidate Class II sources (including two with evidence for a large inner disk hole - see discussion). The Taurus Class II median SED (D’Alessio et al. 1999) is shown for comparison. By examining the SEDs, we have determined approximate regions in the color-color plane corresponding to each of the object classifications, as shown in Figure 2.

The similarity of the SEDs of our new candidates to known PMS objects strongly suggests a PMS origin for most if not all of them. Spectra are needed to definitively weed out non-PMS objects that can also have infrared excesses, such as galaxies or planetary nebulae. Given the significant extinction of the molecular cloud and the relatively small solid angle subtended by the map, we do not expect such contamination to be significant.

4. Discussion

4.1. The Pre-Main Sequence Population

We have created a preliminary inventory of young stellar objects in NGC 7129 using our infrared SEDs. The PMS candidates discussed here comprise only the population located outside of the central reflection nebula, since most of the stars there are hidden by the associated strong extended emission at $24\ \mu\text{m}$. To avoid ambiguity, we have restricted classification to sources detected at $24\ \mu\text{m}$ and at least three of the IRAC bands. A total of 39 objects meet this criterion, out of 49 sources located within the overlapping field of view of the IRAC observations (all of which are detected in at least one IRAC band). The remaining $24\ \mu\text{m}$ sources are worthy of follow-up study. In particular, 7 objects are not detected at 5.8 and $8\ \mu\text{m}$; some of these may be edge-on disk sources, which are predicted to have double-humped SEDs with a large dip between $\sim 3 - 20\ \mu\text{m}$ (D’Alessio et al. 1999).

Of the 39 sources detected in at least four bands, we find that about a third (13) are candidate protostars with circumstellar envelopes. One of these, the source FIRS 2, is probably a Class 0 object, as mentioned above. The other 12, with less extreme colors, are likely Class I objects. Included in this category are two objects with relatively flat spectral slopes (often known as “flat-spectrum” sources), which may be at an evolutionary stage intermediate between Class I and II. Another 18 objects appear to be Class II sources; most if not all of these are probably classical T Tauri stars, given their relatively low infrared luminosities. Six objects have SEDs that are closer to pure photospheres (as also indicated in the color-color diagram), and may be a combination of Class III objects, background

giants, or foreground dwarfs. A few have slightly larger (8-24) colors which may indicate the presence of an optically thin remnant disk. Spectral types are needed to disentangle this group of objects. Finally, three sources have more complicated SEDs that we do not classify; two of them are very faint and appear to the southwest of the reflection nebula, where the extinction is much smaller, and hence may be galaxies.

At first glance, our preliminary results indicate a large fraction of Class I to Class II sources in the outer region of NGC 7129. However, we are missing the core cluster members located inside the reflection nebula. The statistics are also affected to an uncertain degree by completeness at low luminosities. Objects in both classes span a fairly large range of luminosity, but we are likely missing some number of very low-luminosity objects, as well as sources with extreme extinction. The weakest Class II sources we detect are ~ 10 times less luminous than the scaled Taurus median SED that corresponds to a median source luminosity $L \sim 0.8 L_{\odot}$ (see Fig. 3). Similarly low-luminosity protostars do not appear in our classified subsample, probably because their fluxes at the shorter IRAC wavelengths are below our detection threshold. If we add in the pre-main sequence candidates found from the IRAC and near-infrared data alone (Allen et al. 2004; Gutermuth et al. 2004; Megeath et al. 2004), which includes both low-luminosity sources and the central cluster members, we end up with a total of about 20 Class 0/I and 80 Class II objects, resulting in a fraction very similar to that seen in Taurus (Kenyon & Hartmann 1995).

Another interesting result is the spatial distribution of our subsample of 36 classified objects, shown in Figure 4. As is seen for the sample as a whole, most of these objects are located in an arc sweeping north-east-south of the central reflection nebula. This area largely coincides with the densest parts of the molecular cloud, as seen in the optical image and in the gas distribution traced by ^{13}CO and C^{18}O emission (Miskolczi et al. 2001; Ridge et al. 2003). Based on the presence of protostars in this region, we argue that active star formation must be dispersed over a fairly large area (~ 3 pc), and not concentrated in the center as is usually observed. The winds and photoionizing flux of the central B-stars have cleared out most of the molecular material from the central region, preventing formation of new protostars, and may eventually contribute to the cessation of continuing star formation in the surrounding cloud within the next few Myr.

4.2. Transition Objects: Inner Disk Gaps?

We detect three objects whose SEDs show little or no excess at wavelengths $\lesssim 8 \mu\text{m}$, but strong excesses at $24 \mu\text{m}$ (two of these are shown in Fig. 3, objects D2 and D3). Such SEDs are strongly suggestive of disks with inner gaps, such as the 10 Myr-old Class II object

TW Hya (Calvet et al. 2002; also shown in Fig. 3). One of the central goals of circumstellar disk studies is the determination of the timescales for disk evolution, which can constrain the mechanism(s) for planet formation. Evidence so far indicates that primordial disks do not last longer than ~ 10 Myr; however, a large fraction of PMS stars do not show evidence for disks even at ages of 1-3 Myr (Haisch et al. 2001; Gutermuth et al. 2004). Thus, the timescale of the transition from optically thick primordial disk to no disk or regenerative “debris” disk is thought to be fairly short. Objects which show disks with an inner gap may be in this transition phase, with clearing of disk material related to planetesimal accretion. Unfortunately, only a very few such objects have been identified, most of which are older than ~ 1 Myr. Our candidates may provide important new examples of this transition at a very young age.

This work is based in part on observations made with the *Spitzer Space Telescope*, which is operated by the Jet Propulsion Laboratory, California Institute of Technology under NASA contract 1407. Support for this work was provided by NASA through Contract Number 960785 issued by JPL/Caltech.

REFERENCES

- Adams, F. C., Lada, C. J., & Shu, F. H. 1987, *ApJ*, 312, 788
- Allen, L. E., et al. 2004, *ApJS*, this volume
- Calvet, N., D’Alessio, P., Hartmann, L., Wilner, D., Walsh, A., & Sitko, M. 2002, *ApJ*, 568, 1008
- D’Alessio, P., Calvet, N., Hartmann, L., Lizano, S., & Cantó, J. 1999, *ApJ*, 527, 893
- Eiroa, C., Palacios, J., & Casali, M. M. 1998, *A&A*, 335, 243
- Font, A. S., Mitchell, G. F., & Sandell, G. 2001, *ApJ*, 555, 950
- Gordon, K. et al. 2004, *PASP*, in press
- Gutermuth, R. A., Megeath, S. T., Muzerolle, J., Allen, L. E., Pipher, J. L., Myers, P. C., & Fazio, G. G. 2004, *ApJS*, this volume
- Haisch, K. E., Lada, E. A., & Lada, C. J. 2001, *ApJ*, 553, 153
- Hodapp, K. W. 1994, *ApJS*, 94, 615
- Jayawardhana, R., Hartmann, L., Fazio, G., Fisher, R. S., Telesco, C. M., & Piña, R. K. 1999, *ApJ*, 521, L129
- Kenyon, S. J. & Hartmann, L. 1995, *ApJS*, 101, 117

- Kenyon, S. J., Hartmann, L. W., Strom, K. M., & Strom, S. E. 1990, *AJ*, 99, 869
- Lada, C. J. 1987, in *Star Forming Regions*, ed. M. Peimbert and J. Jugaku (Dordrecht: Reidel), p. 1
- Luhman, K. L. & Rieke, G. R. 1999, *ApJ*, 525, 440
- Megeath, S. T. et al. 2004, *ApJS*, this volume
- Miskolczi, B., Tothill, N. F. H., Mitchell, G. F., & Matthews, H. E. 2001, *ApJ*, 560, 841
- Miyake, K. & Nakagawa, Y. 1995, *ApJ*, 441, 361
- Osorio, M., D'Alessio, P., Muzerolle, J., Calvet, N., & Hartmann, L. 2003, *ApJ*, 586, 1148
- Racine, R. 1968, *AJ*, 73, 233
- Ridge, N. A., Wilson, T. L., Megeath, S. T., Allen, L. E., & Myers, P. C. 2003, *AJ*, 126, 286
- Rieke, G. R., et al. 2004, *ApJS*, this volume
- Webb, R. A., Zuckerman, B., Platais, I., Patience, J., White, R. J., Schwartz, M. J. & McCarthy, C. 1999, *ApJ*, 512, L63
- Wilking, B. A., Lada, C. J., & Young, E. T. 1989, *ApJ*, 340, 823

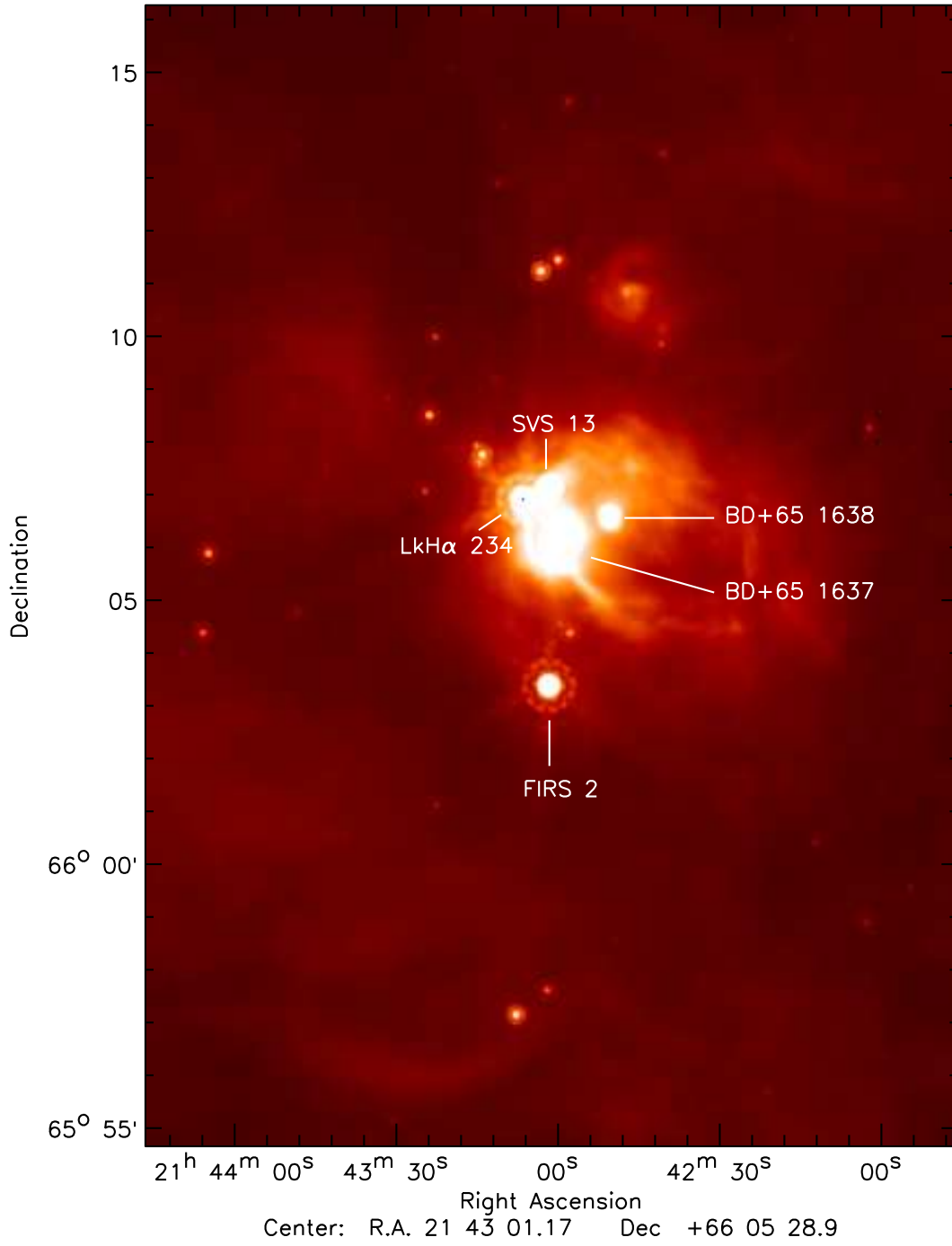


Fig. 1.— A portion of the 24μm scan map of NGC 7129.

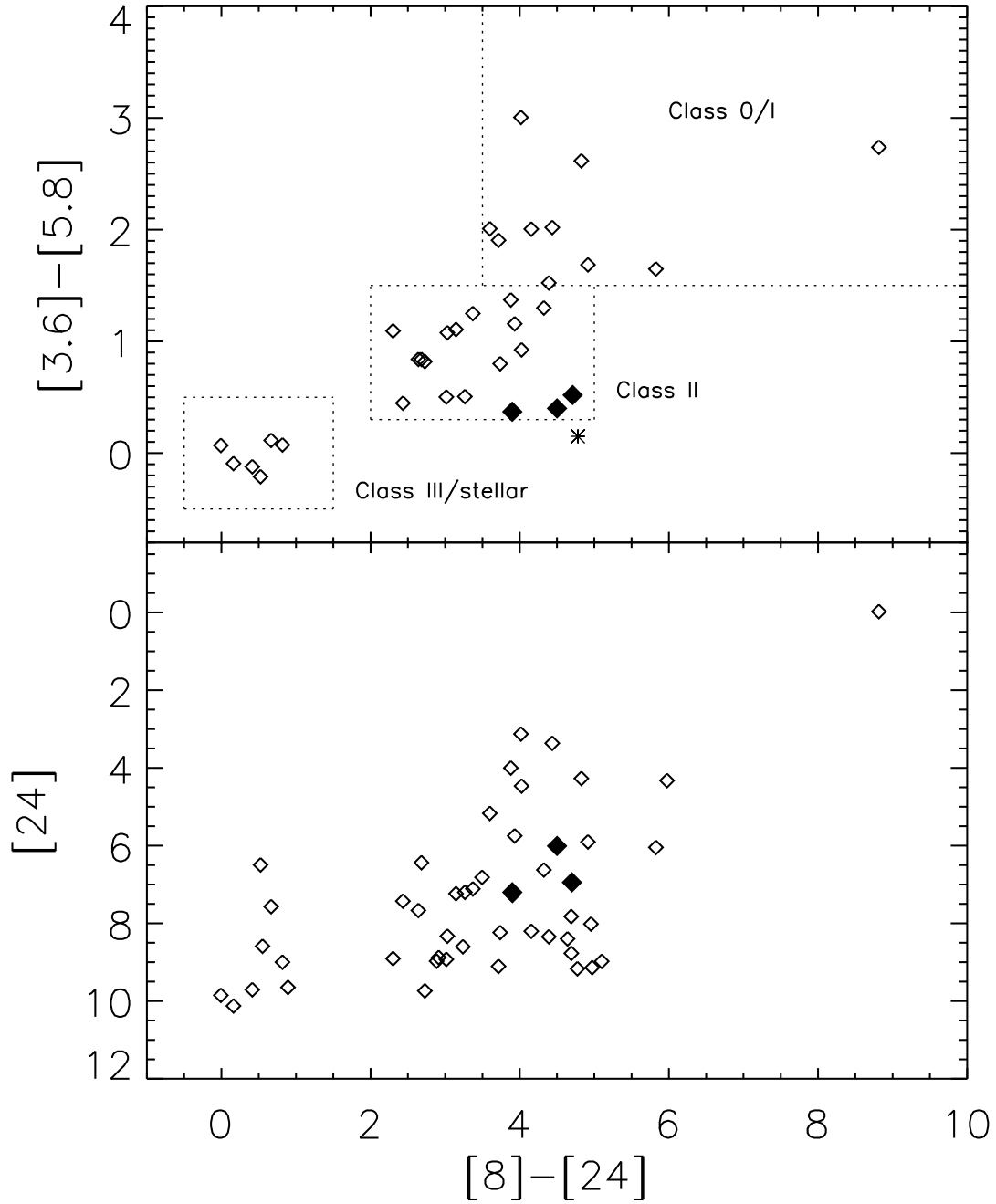


Fig. 2.— Color-color and color-magnitude diagrams for all sources detected in all appropriate bands. Approximate regions for basic object classifications are delineated in the upper panel. The asterisk represents the T Tauri star TW Hya, as determined from IRAC and IRAS $25 \mu\text{m}$ fluxes; solid diamonds are objects with similar SEDs, and may be transition objects with evidence for a gap in the inner disk (see discussion).

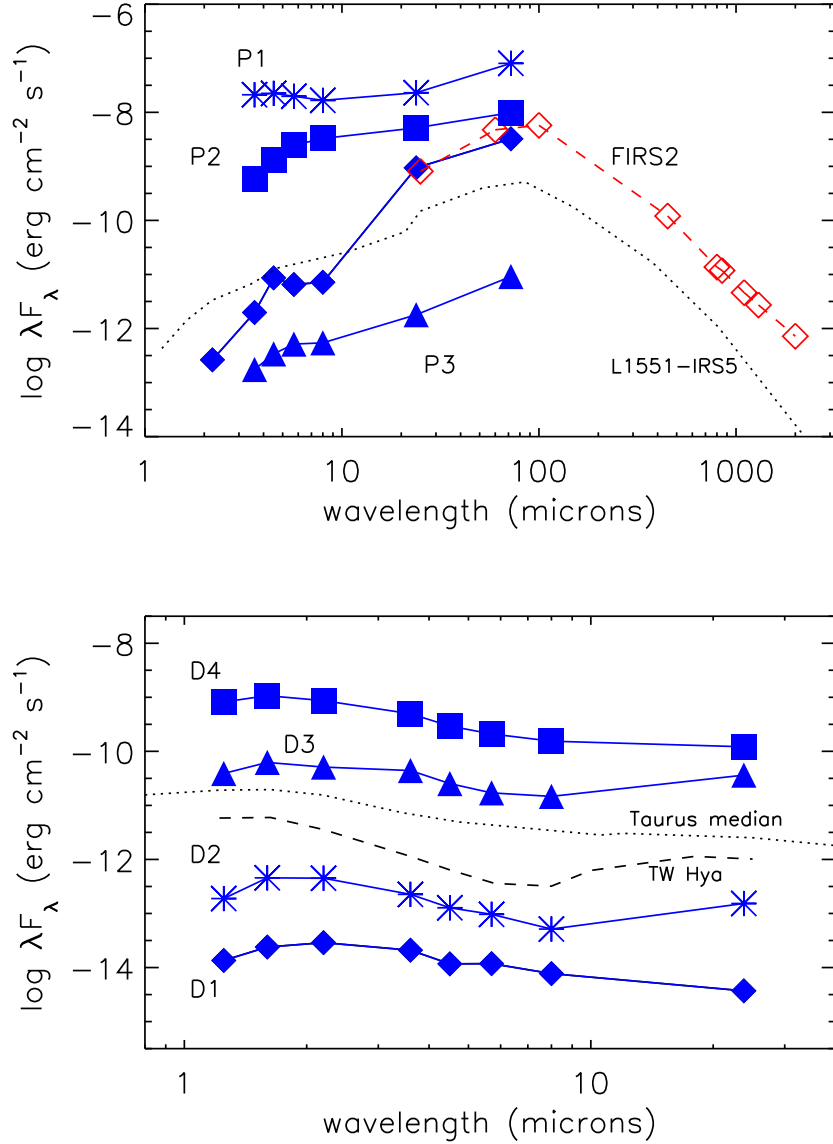


Fig. 3.— Spectral energy distributions for selected sources. (*Top panel*) Protostellar candidates: shown are the 4 sources detected at both 24 and 70 μm . Solid symbols connected by solid lines are IRAC/MIPS fluxes; open symbols connected by a dashed line are IRAS (color corrected assuming a $T = 50$ K blackbody spectrum) and ground-based sub-mm/mm observations of FIRS 2 (Eiroa et al. 1998; Font et al. 2001). The following sources are shifted along the y-axis for clarity: P1 (+3 dex); P2 (+2 dex); P3 (-1 dex). The SED of Taurus Class I object L1551-IRS5, scaled to 1 kpc, is shown with the dotted line (Osorio et al. 2003, and references therein). Note that the fluxes for FIRS 2 at K through 5.8 μm are likely contaminated by shocked emission from outflows (see Gutermuth et al. 2004). (*Bottom panel*) Class II candidates. Source D1 has been shifted by -1.5 dex, D2 by -1 dex, D3 by +2 dex, and D4 by +1 dex along the y-axis. The median SED for Taurus class II objects (D’Alessio et al. 1999) and the SED for TW Hya (data from Webb et al. 1999, Jayawardhana et al. 1999, and IRAS and IRAC observations), both scaled to 1 kpc, are

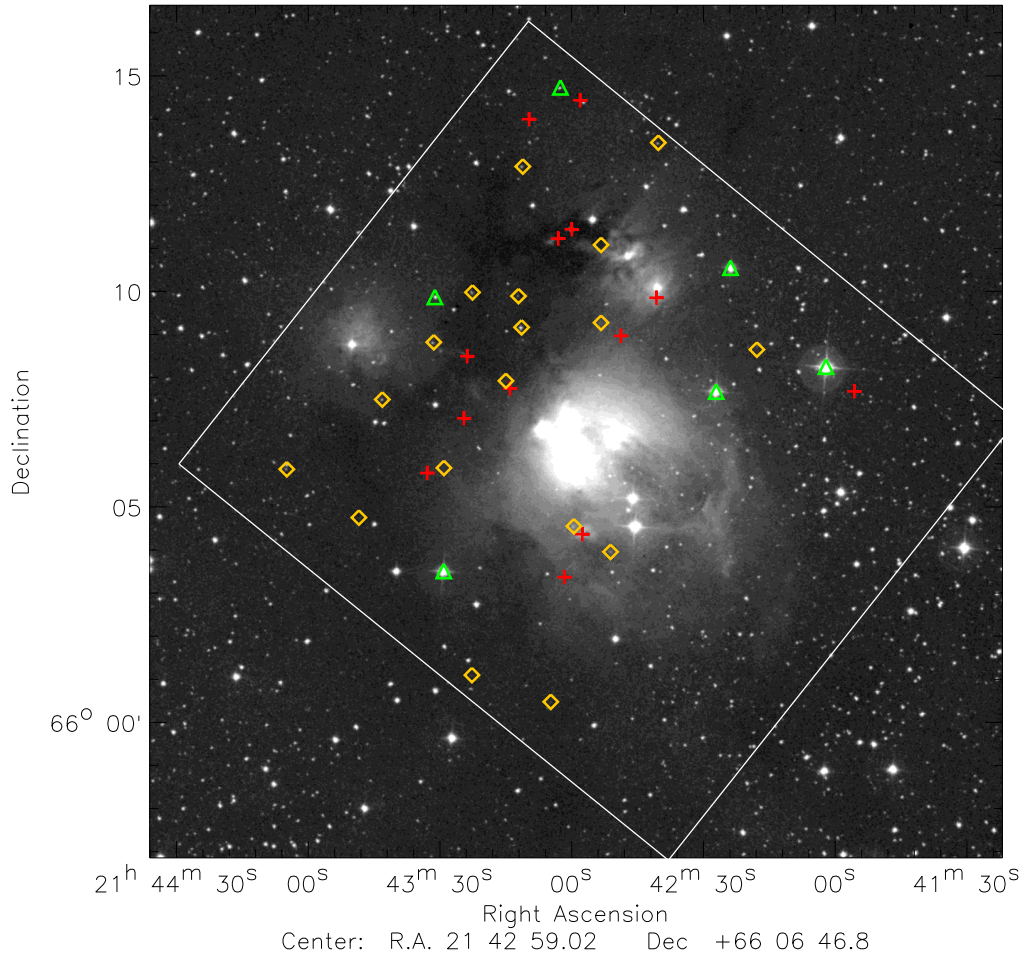


Fig. 4.— Optical DSS image of NGC 7129 overlaid with symbols showing the positions of candidate young stellar objects. Red pluses: Class 0/I objects; yellow diamonds: Class II objects; green triangles: Class III/dwarfs/giants. The overlapping IRAC field of view is shown with a white box.

Table 1. Selected MIPS sources

Object	α (J2000)	δ (J2000)	J	H	K	3.6	4.5	5.8	8.0	24	70
FIRS 2	21 43 01.66	66 03 24.0	16.35	12.67	10.35	9.93	8.79	-0.02	-5.01
P1	21 43 00.00	66 11 28.3	10.10	9.32	8.73	7.88	4.00	-1.00
P2	21 43 03.12	66 11 15.4	11.50	9.88	8.49	7.14	3.13	-1.22
P3	21 43 24.00	66 08 31.6	12.81	11.37	10.19	9.10	4.27	-1.14
D1	21 42 17.52	66 08 40.6	17.38	16.01	15.00	13.86	13.77	13.04	12.47	9.74	...
D2	21 42 53.28	66 11 06.7	15.76	14.06	13.27	12.53	12.43	12.01	11.66	6.95	...
D3	21 43 31.68	66 08 51.0	14.17	13.13	12.55	11.67	11.53	11.16	10.46	7.20	...
D4	21 42 59.51	66 04 35.0	13.27	11.90	11.13	10.44	10.01	9.60	9.12	6.55	...